24AM1F-03

Born Approximated Inverse Scattering Using Beam Basis Functions

T. Heilpern [1], E. Heyman [2]

School of Electrical Engineering, Tel Aviv University, Tel Aviv 69978, Israel.

[1] talhe78@yahoo.com, [2] heyman@tau.ac.il

***Abstract*—We present a novel beam-based inverse scattering algorithm within the Born approximation, utilizing data measured by arrays of point sources and receivers (transducers). In this approach, the measured point-source/receiver data is first converted into a beam-domain data where the source and the receiver arrays are described by phase-space sets of beam waves. The beam-domain data describes the scattering amplitudes "measured" by the receiver beams due to each source beam. In the new inversion approach presented here, the unknown medium is spanned using a basis of beam-waves, and the expansion coefficients are determined by multiplying the beam-domain data with pseudo inverse of the correlation matrix of the beam basis function. The scheme benefits from the sparseness of the beam-domain data and from the spatial localization of the beam spanning functions.**

I. Introduction and Summary

We consider a beam approach for inverse scattering of objects embedded in a background medium. The data is measured by an array of wide-angle (point-like) receivers due to an array of independent wide-angle sources. We consider a monochromatic illumination, although the method may readily be extended to the ultra-wideband (UWB) regime. The inversion is performed within the Born approximation [1].

In the beam approach the data is transformed into the beam domain, and the functions used to expand the object are defined directly in the beam domain. The beam approach has been introduced in [2] together with two imaging algorithms: a backpropagation and correlation algorithm and a MUSIC imaging algorithm.

The present work is based on the same data transformation, but it introduces an alternative inversion approach that utilizes the beam waves as basis functions to span the object. It is shown that within the Born approximation, the beam-domain data represents the projections of the object onto the spanning beam-set. The expansion coefficients are recovered by a filtering type procedure that involves the calculation and (pseudo) inversion of a correlation matrix of the spanning beam functions. This strategy has been presented for general kernels [3] and then for Green's functions kernels [4], [5].

It is shown that the beam approach has certain advantages over the Green's functions approach, mainly due to fact that the beams are localized in space. In the data domain, this implies that the beam-domain data is sparse since it is localized around the source-receiver beam pairs that intersect near the object (Fig. 1). In the processing phase, this localization enables spatial filtering and focusing of the data since one may *a priori* eliminate source and receiver beams that do not illuminate a particular domain of interest (DoI). It follows that the number N_b of beams used to span the object is small relative to the number of transducers in the source/receiver arrays, leading to a significant reduction in the numerical complexity of the algorithm since the correlation matrix that has to be calculated and inverted has N_b^4 elements.

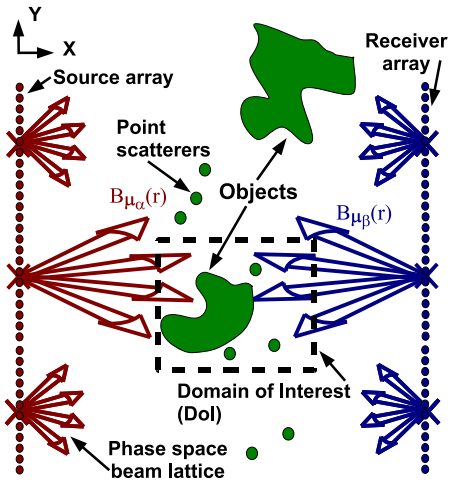

Fig. 1. Physical configuration: The 1D source and receiver arrays of point-like transducers are located parallel to the y-axis. The source and receiver fields are converted into the beam domain, schematized by the wide arrows. The scatterers are marked in green. The only non-negligible terms in the beam-domain data matrix are those corresponding to source-receiver beam pairs that intersect near the targets.

II. Physical configuration and the Born approximation of the measured data

We consider the 2D configuration in Fig. 1 where an unknown object O is located in a finite support domain V in the (x, y) plane. The medium is probed by P *independent* sources at $\boldsymbol{\alpha}_p = (x_{\alpha_p}, y_{\alpha_p})$, $p = 1, \ldots, P$, and Q receivers at $\boldsymbol{\beta}_q$, $q = 1, \ldots, Q$. For simplicity it is assumed that the sources and receivers are point-like with omni-directional radiation pattern, and are arranged in linear equi-spaced arrays parallel to the y-axis. These arrays can be on two opposite sides of the target domain, as schematized in Fig. 1, or be on the same side (representing transmission or reflection mode imaging, respectively). Henceforth, Constituents associated with the source or the receiver arrays will be tagged by subscript α

or β, respectively. Furthermore, a harmonic time-dependence $e^{-i\omega t}$ is assumed and suppressed throughout.

The scattering data is arranged in a *data matrix* $\mathbf{K}\,[Q\times P]$ such that K_{qp} is the field recorded at the q-th receiver due to the p-th source excited at a unit amplitude.

The object is characterized by the contrast function $O(\mathbf{r}) = n^2(\mathbf{r}) - n_0^2(\mathbf{r})$ where $n(\mathbf{r})$ is the object's refractive index and $n_0(\mathbf{r})$ is the known background. The weak scattering approximation of the data matrix is given by

$$\tilde{K}_{qp} \approx k^2 \int_V d^2r G_0(\boldsymbol{\beta}_q, \mathbf{r}) O(\mathbf{r}) G_0(\mathbf{r}, \boldsymbol{\alpha}_p) \tag{1}$$

where G_0 is the Green's function in the background and $k = \omega/c$ is the free space wavenumber. Here and henceforth an over-tilde tags expressions within the Born approximation, assuming that $O \ll n_0^2$ and $kOD \ll 1$ where O and D are measures of the magnitude and of the support of $O(\mathbf{r})$. Defining the "steering vectors"

$$\mathbf{g}_\alpha(\mathbf{r}) = \left[G(\mathbf{r}, \boldsymbol{\alpha}_1), ..., G(\mathbf{r}, \boldsymbol{\alpha}_{N_\alpha})\right]^t \tag{2a}$$

$$\mathbf{g}_\beta(\mathbf{r}) = \left[G(\boldsymbol{\beta}_1, \mathbf{r}), ..., G(\boldsymbol{\beta}_{N_\beta}, \mathbf{r})\right]^t, \tag{2b}$$

with the superscript t denoting matrix transpose, we may express (1) in a more compact outer product format

$$\tilde{\mathbf{K}} \approx k^2 \int_V d^2r\, \mathbf{g}_\beta(\mathbf{r}) O(r) \mathbf{g}_\alpha^t(\mathbf{r}). \tag{3}$$

III. The UWB phase-space beam basis

In this section we present the data transformation into the beam domain. We consider the UWB phase-space beam-set of [6]. These beams emerge from a discrete set of points y_m in the source/data domain and in a discrete set of directions ϕ_n associated with the wavenumbers $k_{y_n} = k\sin\phi_n$. The set is structured upon a Cartesian lattice in the (y, k_y) phase-space such that $(y_m, k_{y_n}) = (m\bar{y}, nk\bar{\xi}_y$, with $(m,n) \in \mathbb{Z}^2$. The unit-cell dimensions $(\bar{y}, \bar{\xi}_y)$ are chosen to provide an overcomplete coverage of the phase space such that $k\bar{y}\bar{\xi}_y = 2\pi\nu$ where $\nu < 1$ is the so called overcompleteness parameter. For UWB applications, $(\bar{y}, \bar{\xi}_y)$ are chosen to be frequency independent.

Using this overcomplete phase-space set of beams, the field $u(\mathbf{r})$ due to any source distribution along the y-axis may be expressed as

$$u(\mathbf{r}) = \sum_{\boldsymbol{\mu}} a_{\boldsymbol{\mu}} B_{\boldsymbol{\mu}}(\mathbf{r}), \qquad \boldsymbol{\mu} = (m,n) \in \mathbb{Z}^2 \tag{4}$$

where $B_{\boldsymbol{\mu}}(\mathbf{r})$ are the beam propagators, $a_{\boldsymbol{\mu}}$ are the expansion coefficients (the beam amplitudes), and $\boldsymbol{\mu}$ is an index. The phase space beam summation representation in [6] has the following favorable properties:

(i) The beam lattice defined by the initiation points and directions (y_m, ϕ_n) is *frequency independent*. This implies that only a single set of beams needs to be tracked in the medium and then used for all frequencies. Specifically, it is sufficient to track only the beam propagators (or back-propagators) that pass through the domain of interest (DoI).

(ii) The algorithm utilizes the so called iso-diffracting Gaussian beams (ID-GB) whose propagation parameters can be calculated analytically in inhomogeneous media. The ID parametrization implies that the beamwidth is scaled with frequency such that the propagation parameters are frequency independent, so that they need to be calculated only once and then used for all frequencies. This set of beams, when judiciously chosen, provides the *snuggest* beam representation of the field for all frequencies.

Using the representation in (4), the steering vector $\mathbf{g}$ in (2) may be expressed by the corresponding beam-base vector $\mathbf{b}(\mathbf{r})$ via the matrix transformation

$$\mathbf{g}(\mathbf{r}) = \mathbf{A}\mathbf{b}(\mathbf{r}), \qquad \mathbf{b}(\mathbf{r}) = \left[B_1(\mathbf{r}), ..., B_{N_b}(\mathbf{r})\right]^t, \tag{5}$$

where N_b is the number of beams needed to describe the field of the transducers array (i.e., the beam initiation points typically cover the array). Closed form expressions for the matrix elements $A_{p,\mu}$ have been derived in [2], [7]. They depend on the array parameters (the inter-element spacing d) and of the beam set (the overcompleteness and the beam-collimation).

In the proposed algorithm, the data is first converted into the beam domain. We need therefore to find an inverse relation to (5) in the form

$$\mathbf{b}(\mathbf{r}) = \mathbf{M}\mathbf{g}(\mathbf{r}), \tag{6}$$

where $\mathbf{M}$ is a matrix that can be calculated. It can be shown that if the elements of $\mathbf{b}$ are sufficiently far from the endpoint of the source array then $\mathbf{M} \approx \gamma_0 \bar{\mathbf{A}}^\dagger$, where $\bar{\mathbf{A}}$ is the corresponding sub matrix of $\mathbf{A}$, and γ_0 is a constant.

Using the transformation (6), the measured point-transducers data matrix is converted into the beam-domain data matrix

$$\mathbf{K}_b = \mathbf{M}_\beta \mathbf{K} \mathbf{M}_\alpha^t, \tag{7}$$

where the subscripts α, β tag the source/receiver matrixes, as mentioned earlier. Substituting (3) into (7) leads to the weak scattering model of $\mathbf{K}_b$,

$$\tilde{\mathbf{K}}_b \approx k^2 \int_V d^2r\, \mathbf{b}_\beta(\mathbf{r}) O(\mathbf{r}) \mathbf{b}_\alpha^t(\mathbf{r}). \tag{8}$$

Specifically, the $(\boldsymbol{\mu}_\beta, \boldsymbol{\mu}_\alpha)$ element in $\tilde{\mathbf{K}}_b$ is given by

$$\left[\tilde{K}_b\right]_{\boldsymbol{\mu}_\beta, \boldsymbol{\mu}_\alpha} \approx k^2 \int_V d^2r\, B_{\boldsymbol{\mu}_\beta}(\mathbf{r}) O(r) B_{\boldsymbol{\mu}_\alpha}^t(\mathbf{r}), \tag{9}$$

i.e., the field of the $\boldsymbol{\mu}_\alpha$ source-beam that is scattered by the object and then sensed by the $\boldsymbol{\mu}_\beta$ receiver-beam. This observation implies that $\mathbf{K}_b$ is sparse since its elements are non-negligible only for source/receiver beam-pairs $(\boldsymbol{\mu}_\beta, \boldsymbol{\mu}_\alpha)$ that intersect near the scattering object. This localization also enables spatial filtering and focusing of the data, since one may *a priori* eliminate rows and columns corresponding to source and receiver beams that do not illuminate the DoI.

IV. Beam-based inverse scattering algorithm within the Born approximation

The inversion approach follows the method used for general kernels in [3] and for Green's functions kernels in [4]. here, however, we use beam-waves kernels.

For simplicity we re-order the data matrix $\mathbf{K}_b$ of (7) as a data vector $\mathbf{k}_b$ (for example by taking column after column from $\mathbf{K}_b$)

$$\left[k_b\right]_l = \left[K_b\right]_{\boldsymbol{\mu}_\beta,\boldsymbol{\mu}_\alpha}, \quad l = 1...L^{\text{DoI}}, \quad L^{\text{DoI}} = N_\alpha^{\text{DoI}} N_\beta^{\text{DoI}} \tag{10}$$

where $N_{\alpha,\beta}^{\text{DoI}}$ are the number of source/receiver beams which pass through the domain of interest (DoI) respectively. Next, we define the L^{DoI} spanning functions

$$F_l(\mathbf{r}) = \begin{cases} B^*_{\boldsymbol{\mu}_\alpha}(\mathbf{r}) B^*_{\boldsymbol{\mu}_\beta}(\mathbf{r}) & \text{if } \mathbf{r} \in V, \\ 0 & \text{otherwise.} \end{cases} \tag{11}$$

Inserting (10) and (11) into (9) yields

$$\left[k_b\right]_l = \int_V d^2r\, F_l^*(\mathbf{r}) O(\mathbf{r}) \equiv \langle F_l(\mathbf{r}), O(\mathbf{r}) \rangle \tag{12}$$

which implies that the data matrix expresses the projection of the object onto the subspace spanned by $F_l(\mathbf{r}), \quad l = 1...L^{\text{DoI}}$.

The solution involves only the $L^{\text{DoI}} \ll L = (N_\alpha N_\beta)$ beam-pairs passing through the object domain V, and the data vector $\mathbf{k}_b$ is also truncated to contains only the relevant L^{DoI} elements. The minimum $\mathbb{L}^2$ norm solution of the inverse scattering problem within the Born approximation is given therefore as a sum of the $F_l(\mathbf{r})$ functions

$$\hat{O}(\mathbf{r}) = \sum_{l=1}^{L^{\text{DoI}}} c_l F_l(\mathbf{r}) = \mathbf{c}^t \mathbf{F}(\mathbf{r}), \tag{13}$$

where $\mathbf{c}$ and $\mathbf{F}$ are the vector of c_l and F_l. Substituting (13) into (12) leads into the matrix equation

$$\boldsymbol{\Phi}\mathbf{c} = \mathbf{k}_b, \quad \Phi_{l,l'} = \langle F_l, F_{l'} \rangle = \int_V d^2r F_l^*(\mathbf{r}) F_{l'}(\mathbf{r}). \tag{14}$$

The matrix $\boldsymbol{\Phi}$ is formed by an overlapping of 4 beams hence it is sparse and consists only of terms corresponding to beams passing in the image domain. In contradistinction, the Green's functions matrix $\boldsymbol{\Pi}$ matrix in [4] is both larger and non sparse.

A solution of (14) may expressed in terms of the least square pseudo-inverse of $\boldsymbol{\Phi}$ viz

$$\hat{\mathbf{c}} = \boldsymbol{\Phi}^{-I}\mathbf{k}_b, \quad \{\}^{-I} = \text{Pseudo inverse}, \tag{15}$$

and the object is given by

$$\hat{O}(\mathbf{r}) = (\boldsymbol{\Phi}^{-I}\mathbf{k}_b)^t \mathbf{F}(\mathbf{r}). \tag{16}$$

V. Numerical Example

As a first example of this new approach we consider a 2D example with a homogeneous medium and small (point) scatterers. The data satisfies the Born approximation (no multiple scattering). Random noise was added to each element of the data matrix.

Referring to Fig. 2, we consider a 300 elements point-transducers array located along the y axis with inter-element spacing $d = 1$ (black points on the left hand side of the figure). The wavespeed in taken to be $c = 1$. We use a single frequency $\omega = \pi$, i.e $d/\lambda = 0.5$, which is the highest frequency with no array grating-lobes. The imaging domain is a rectangle of

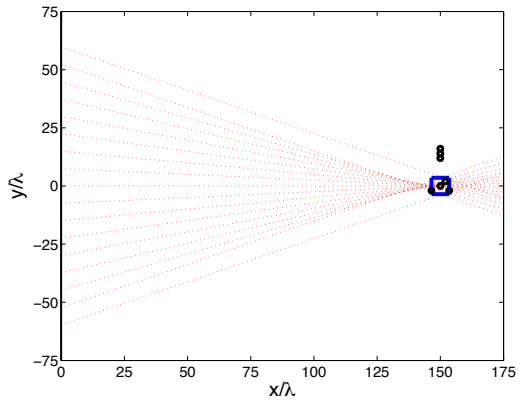

Fig. 2. Physical configuration for the numerical example: The same 300 point-transducers array along the y axis is used excitations and receivers (black dots on the left hand side of the figure). 4 point targets marked with • are located within the DoI marked by the blue rectangle, while 3 targets are located outside the DoI. Also shown are the axes of the 17 beams that pass through the DoI.

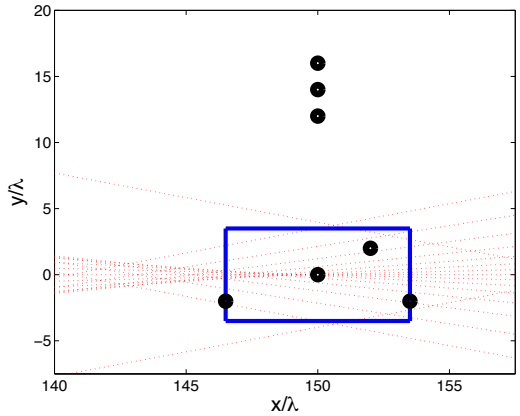

Fig. 3. Physical configuration for the numerical example: Zoom on the targets domain

size $[20\lambda \times 25\lambda]$, and the DoI is the $7\lambda \times 7\lambda$ rectangle marked by the blue rectangle. There are 4 point targets in the DoI at $(x/\lambda, y/\lambda) = (146.5, -2), (150, 0), (152, 2), (153.5, -2)$, and 3 point targets at $(150, 12), (150, 14), (150, 16)$ outside the DoI.

Referring to the phase-space beam expansion in [2], [6], we choose beams with a collimation length $b = 300$ and an overcompleteness parameter $\nu^{-1} = 2.5$. Following the formulation in [6], one finds that the distance between the beam initiation points is $\bar{y} = 14.95$, yielding 17 initiation points within the array, and 41 visible spectrum directions ϕ_n for each y_m, i.e., a total of $N_\alpha = N_\beta = 17 \times 41 = 697$ beams. However, only $N_\alpha^{\text{DoI}} = 17$ beams pass within the DoI; their axes are marked in Fig. 2 with dotted red lines.

We add noise to the data by multiplying the elements of $\mathbf{K}$ by a noise term

$$K_{qp} = K_{qp}^0(1 + n_c), \quad n_c = n_r + in_i, \quad n_r, n_i \sim \mathcal{N}(0, \sigma_N^2), \tag{17}$$

K_{qp}^0 is the noise-free term and n_c is a complex noise where

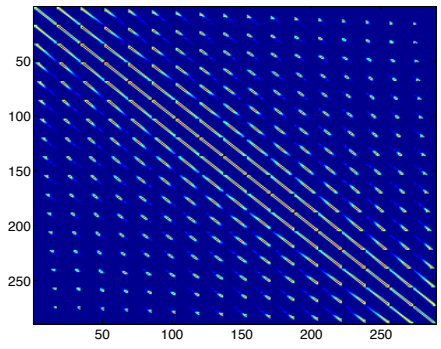

Fig. 4. $|\mathbf{\Phi}|$

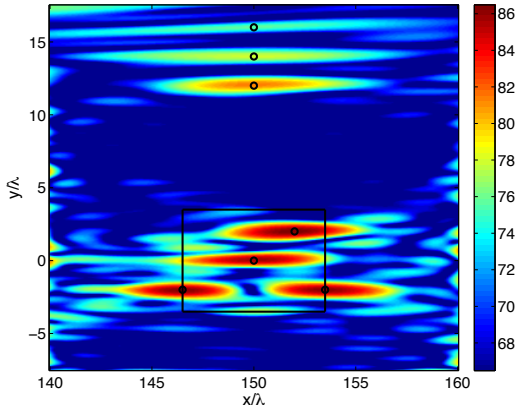

Fig. 5. $|\hat{O}(\mathbf{r})|$, No Noise

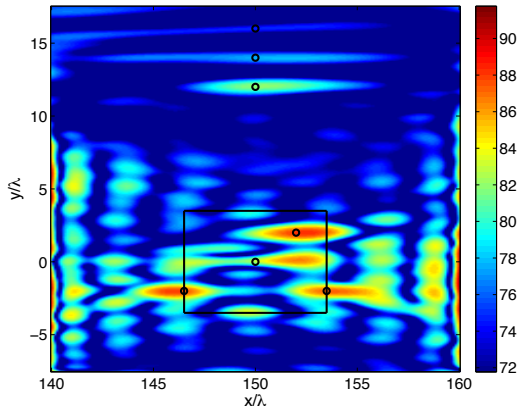

Fig. 6. $|\hat{O}(\mathbf{r})|$, S/N=50dB

both n_r and n_i are normal with zero mean and standard deviation σ_N. Thus $|n_c|$ has a Rayleigh distribution with mean $\sigma_N\sqrt{\pi/2}$ and standard deviation $\sigma_N\sqrt{2-\pi/2}$. n_c were randomly selected for each element K_{qp}. We chose a noise level of $\sigma_N = 0.0025$, corresponding to S/N$= 20\log\sigma_N^{-1}\sqrt{2/\pi} =$ 50dB. The beam based data matrix is generated using (7).

In Fig. 4 we show the $[L^{\text{DoI}} \times L^{\text{DoI}}]$ correlation matrix $\mathbf{\Phi}$ of (14), with $L^{\text{DoI}} = (N_\alpha^{\text{DoI}})^2 = 17^2$. The diagonals pattern is clearly noted, suggesting that the number of L^{DoI} spanning functions can be further reduced. Note also that using a similar approach but with Green's functions G instead of beams B requires the calculation of a $[P^2 \times P^2]$ correlation matrix with $P = 300$, which may be prohibitively large.

In Figs. 5 and 6 we depict the images of the objects in the DoI calculated via (16) using, respectively, noiseless data and noisy data with S/N$= 50dB$.

One observes that the algorithm provides good cross-range resolution at the specified noise level, and even some range resolution. Clearly, range-resolution in this algorithm requires UWB data. Note also that targets outside the DoI are weak since we a priori excluded beams that do not pass in the DoI.

REFERENCES

[1] A. C. Kak, Malcolm Slaney, *Principles of Computerized Tomographic Imaging,* IEEE Press, 1988.

[2] T. Heilpern, *Beam Based Imaging.* Ph.D. thesis, Tel-Aviv University, 2012.

[3] S. Twomey, "Information content in remote sensing," *Applied Optics*, **13(4)**, 942–945, 1974

[4] A.J. Devaney, M. Dennison, "Inverse scattering in inhomogeneous background media," *Inverse Problems*, **19**, 855–870, 2003

[5] M. Dennison, A.J. Devaney, "Inverse scattering in inhomogeneous background media: II. Multi-frequency case and SVD formulation," *Inverse Problems*, **20**, 1307–1324, 2004

[6] A. Shlivinski, E. Heyman, A. Boag, and C. Letrou, "A phase-space beam summation formulation for ultra wideband radiation," *IEEE Trans. Antennas Propagat.*, **52**, 2042–2056, 2004.

[7] T. Heilpern, A. Shlivinski, and E. Heyman, "Beam-based back-propagation imaging," *Proc. of the International Conference on Electromagnetics in Advanced Applications (ICEAA'09)*, Turin, Italy, Sept. 2009.